Journal of Engineering Science and Technology
Vol. 15, No. 4 (2020) 2248 - 2269

MULTI-GAIT STRATEGIES FOR A QUADRUPEDAL STARFISH SOFT ROBOT INCORPORATING MOTOR-TENDON ACTUATOR

M. MUNADI[1,*], MOCHAMMAD ARIYANTO[1],
JOGA D. SETIAWAN[1], TOMOHIDE NANIWA[2]

[1]Dept. of Mechanical Engineering, Faculty of Engineering, Diponegoro University,
Jl. Prof. Soedarto, Tembalang 50275, Semarang, Indonesia
[2]Dept. of Human and Artificial Intelligent Systems, University of Fukui
3-9-1 Bunkyo, Fukui 910-8507, Japan
*Corresponding Author: munadi@lecturer.undip.ac.id

Abstract

The majority of untethered robots are developed using rigid material. The use of rigid material has several limitations, one of which is the stability of the robot when moving/walking in difficult terrain. This is a challenge in developing robots that can adapt to unpredictable areas or complex work environments. One solution offered is the development of soft robots. Soft robots have the advantage of flexibility across complex environments. However, most untethered legged soft robots are driven by pneumatic actuators that have slower and less precise responses, and soft robot surfaces are prone to tearing and breaking. In this study, the development of soft robots using motor-tendon actuators was carried out. Multi gait pattern strategies are developed for controlling the walking gait of the robot. Undulating and crawling gaits are selected as the main gaits of the robot. The gaits are generated using the sixth order Fourier series. After the gait strategy is developed and embedded in the robot, various tests are performed to test the robot's walking movements such as forward, backward, and turning on smooth and rough surfaces. The tests are performed to determine the ability of the robot to pass through small and impassable obstacles. The total robot weight is 545 grams and can carry loads up to 400 grams. Based on testing the motion strategy that has been developed using the Fourier series, the robot is able to walk on flat terrain with smooth or rough surfaces, the robot also manages to pass obstacles such as small and impassable obstacles. The range of wireless cameras that can be achieved is 60 meters, while the range for wireless robot control is 46 meters.

Keywords: Gait strategy, Motor-tendon actuation, Multi-gait pattern, Soft robot.

1. Introduction

Robot technology is growing rapidly. This is due to the role of robots that can assist human work, especially in dangerous environments, such as in the areas affected by nuclear radiation, bomb disposal, and others. More robots are implemented in the industrial revolution 4.0 that put forward the role of automation and internet of things in the new era of industry today. In its development of the robot in terms of utilized material, the traditional robot uses rigid or hard material. Although hard robots have made great progress, robots that use rigid material still have many limitations. Some of these limitations are mechanical and include instability when moving on difficult terrain. Some hard robots have a limited range of motion and complex control systems. In addition, robots with rigid material types are also limited to certain fields and terrains [1].

To overcome the shortcomings of the hard robot, researchers began to develop robots with elastic/soft material or commonly called soft robots. Soft robots have a good approach to adapt to complex environments. Thus, the use of sensors and modern control systems can be minimized [2]. The development in the direction of soft robots is due to the better understanding of mechanical systems, and the merging of biology to the robot system. A series of soft robot units is defined as an elastic structure that has an unlimited degree of freedom with actuation and is distributed throughout the soft robot structure [3]. In most locomotion of soft robots, pneumatic actuators [4-7] and shape memory alloy (SMA) actuators [8-13] are commonly widely used.

For pneumatic actuators, the robot can be controlled at a distance, but the movement is still slow, and the dimensions are too large, with a length reaching 65 cm [6]. The SMA spring is used as the artificial actuator, in which it can be easily designed and controlled according to the displacement and force requirements [8]. Then, another researcher points out that the efficiency and flexibility of multi-material 3D printing in tailoring the deformed shape of the SMA based soft actuators, which cannot be accomplished using conventional manufacturing methods such as moulding [9]. Other researchers have also used SMA wire for the starfish robot [10] and SMA spring as soft actuators for bionic structure as the artificial hydraulic water vascular system of starfish robot [11].

The locomotion analysis and optimization of actinomorphic soft robots, which are composed of soft arms actuated by shape memory alloy wires are presented in [12]. It is also almost similar to [13] that presented an integrated development of locomotive soft robot platform with multi-limb bodies actuated by shape memory alloys (SMA). Further, soft robots that can crawl or walk using both types of actuators are less suitable because of their slow movements and require many additional components [14]. Therefore, this study selects a motor-tendon type actuator because it is theoretically safer to use, and its movements are more precise, stronger and faster [15, 16].

Motor-tendon actuators were implemented in the soft robot locomotion to control the deformation of the soft body for crawling locomotion [16-21]. By implementing a motor-tendon actuator, a research team has succeeded to develop a single segment worm robot capable of moving forward locomotion [17]. A soft robot incorporated a motor-tendon actuator has been developed by controlling the deformation of the soft body as robot locomotion behavior [18].

A caterpillar-inspired soft robot has been built by using a soft viscoelastic foam. The robot was actuated by the motor-tendon actuator and able to mimic the gait of a caterpillar. It can adapt to a range of environments by using its flexible body [19]. Soft robot locomotion by using body shape deformation can be achieved by incorporating a dual motor-tendon actuator. The proposed robot can crawl at 13 mm/s and turning at 9º/s [20]. Body shape deformation was used as the main locomotion of a soft crawling robot actuated by the motor-tendon actuator. The robot was able to turn left and turn right [21].

Most of the soft robot terrestrial locomotion that have been previously developed and actuated by motor-tendon actuator utilized deformation of the soft body for crawling locomotion. In this study, the proposed untethered starfish-like soft robot incorporated motor-tendon actuator is expected to be able to overcome the problems in both types of pneumatic and SMA actuators such as unable to generate large force due to its elastic structure [22].

Using compliant found in soft robot structure, the motor-tendon actuator is utilized for controlling the bending angle of the developed soft leg. The resulted bending angle with respect to the given servomotor command is conducted experimentally. Gait generations based on undulating and crawling are designed using the Fourier series. The acquired gait pattern is embedded in the Arduino microcontroller. The developed robot is commanded to walk in terrains with small and impassable obstacles. A joystick is included in the robot system to assist the pilot to drive the robot and the wireless camera to observe the condition around the robot.

2. Design and Manufacture

For the mechanical design of terrestrial locomotion, the robot drive is inspired by a starfish's leg. Starfish can walk by bending and straightening their legs to crawl on the ground. A motor-tendon actuator is suitable when applied to this mechanism. To move the soft leg of the robot, the servomotor pulls the tendon connected to the tip of the soft leg from the robot to produce bending motion. The bending and unbending motion of the soft legs can be used for the locomotion of the proposed soft robot. The motion to straighten/unbend the robot's leg can be performed by using the elasticity of the material and structure of the soft leg.

The design developed in this study is intended for the purpose of walking locomotion, so an untethered system is needed [23]. Therefore, it must be able to combine a set of functional elements (body, power supply system, gait motion, etc.). At the design stage, several quadrupedal starfish soft robot configurations have been studied. This is performed to find the best design so that the quadrupedal starfish soft robot is able to meet the research objectives.

In this study, it is expected that the quadrupedal starfish soft robot is able to move in various directions. The proposed soft robot must be able to fulfil a number of important points, namely having a form with an X configuration, minimalist body design, being able to walk forward, turning, and backward, and in real-time to update the visual conditions in its path. The quadrupedal starfish soft robot design is shown in Fig. 1. The soft robot body is designed so that the centre of gravity (CoG) is in the centre of the body of the soft robot.

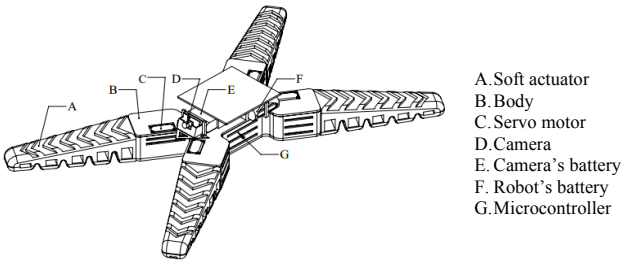

Fig. 1. Quadrupedal starfish soft robot design.

2.1. Design and leg manufacture

The casting process was chosen for manufacturing soft leg actuators with RTV-52 silicone rubber material. In the manufacturing process of the actuator and mold design, there are a number of things that need to be considered including aspects of functionality, ease of casting, material quality, composition, and the effect of actuator angle/bending. In this study, four initial designs of soft legs are proposed and manufactured. The selection of the most suitable soft leg for robot locomotion is assessed using a decision matrix as summarized in Table 1. The four manufacturing results of the initial soft leg motor-tendons are shown in Fig. 2.

After the soft legs are manufactured as shown in Fig. 2, an appropriate selection is made according to the robot. The basis for soft leg selection is actuator mass, dimensions, and stiffness. The three parameters are applied in Table 1 where the value of 5 is the highest value and 1 is the lowest value. Based on Table 1, the soft leg d design has the highest total weight, so soft leg d is applied to the proposed robot.

Table 1. Soft leg design decision matrix.

Parameters	Weight	Soft leg a	Soft leg b	Soft leg c	Soft leg d
Mass	0.3	4	4	5	3
Dimension	0.3	3	4	3	5
Stiffness	0.4	2	3	3	4
	1	2.9	3.6	3.6	4

Figure 2 reveals the comparison of the four types of soft tendon actuators. The designs from (a) to (d) have dimensions of 120 x 30 x 33 mm each; 115 x 36 x 32 mm; 100 x 30 x 33 mm; 116 x 35 x 30 mm. The mass of the four soft tendon actuators weighing 57 grams each; 61 grams; 50 grams; and 68 grams. The material used in this research is RTV-52 silicone rubber. The composition of silicone rubber to the catalyst is 35:1. With this comparison, the composition of the material can be processed without worrying that it will harden before being poured into a mold because it has a long enough pot life which ranges from 18-20 minutes. The effect of this material composition will affect the curing time during the casting process that can reach 10 hours. From the four types of actuators, the selected actuator (d) as a quadrupedal starfish soft robot component. Soft tendon actuator (d) was chosen because it suits the needs of soft robot motion both in terms of dimensions, mass, and flexibility. In terms of dimensions, the soft robot in this research requires a minimalist dimension. In terms of mass, soft robots require soft tendons with light mass but still proportional to the design. In terms of the degree of curvature, it

requires a large curvature that able to approach the given tensile angle. In this case, the soft tendon (d) is able to meet the need for a bending angle at an angle of 120º. The previous design, manufacturing, and test of the soft leg can be found in reference [24].

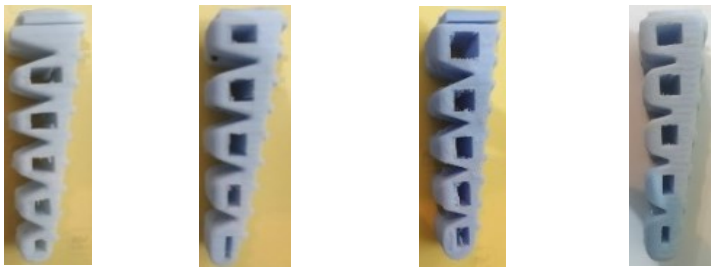

(a) First legs. **(b) Second leg.** **(c) Third leg.** **(d) Fourth legs.**

Fig. 2. Soft leg actuator design and casting results.

To find out the level of uniformity of the bending angle produced on the soft legs, an input angle is given on the servo motor to pull the soft leg in order to form a bending motion. The test was conducted on all four soft legs. The test was carried out with an input angle on the servomotor from 0º to 150º. The resulted bending angles on the four soft legs are depicted in Fig. 3. Based on the test results, there are no significant differences among the given input angles of the servomotor. The formed bending angle of the soft leg is utilized as the locomotion of the proposed robot.

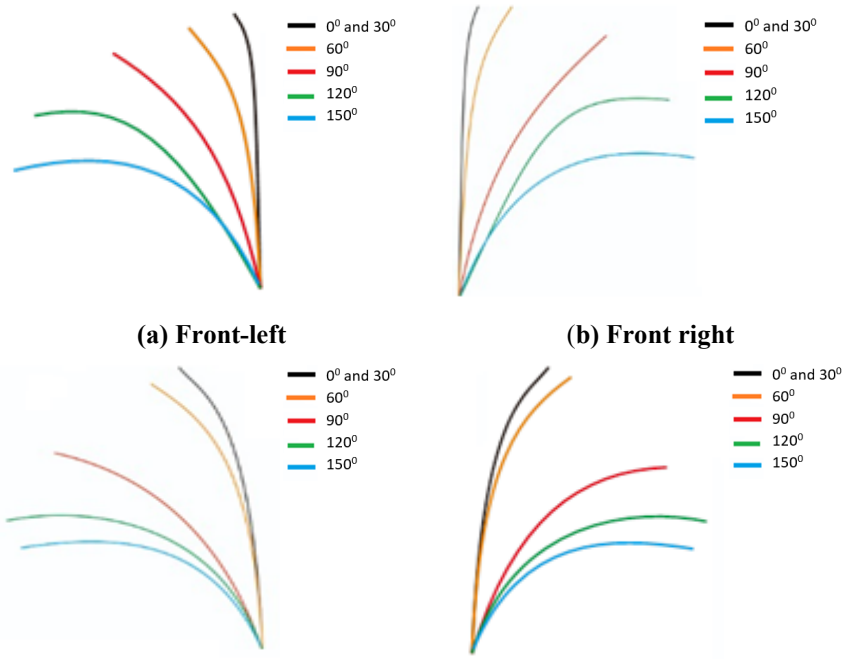

(a) Front-left **(b) Front right**

(c) Rear-right **(d) Rear-left**

Fig. 3. Resulted bending angle with given servomotor angle input.

2.2. Body design

In this study, three 3D robot body models were designed and manufactured with a 3D printer. Material PLA (Polylactic Acid) was chosen as the main material of the robot body because it has good mechanical properties and affordable prices. All three designs have their respective specifications that meet the needs of a soft tendon. Figure 4 shows the manufacturing results of the soft robot body.

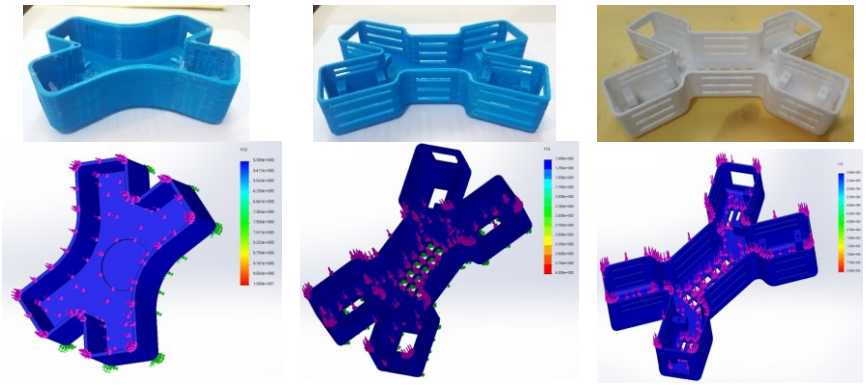

(a) First design **(b) Second design** **(c) Third design**

Fig. 4. Quadrupedal starfish soft robot body results.

The selection process is carried out based on the strengths and weaknesses of each body. Design (*a*) has a larger space with a dimension of 154 x 112 x 40 mm and a wall thickness of 3 mm. As a result of the thickness of the wall of the design (*a*) causes the mass of the design to be heavier, reaching 77 grams. With these dimensions, the body (*a*) can accommodate volume as much as 398 cm^3. Design (*a*) tends to make components that will be inserted into the body become hot quickly. This is because the body (*a*) is designed with a closed shape on all parts except the locked actuator.

Design (b) has dimensions of 157 x 100 x 30 mm with a wall thickness of 1.6 mm. The dimension and thickness are smaller than the design (*a*) causes this design to have a lighter mass. The design mass (*b*) only reaches 39 grams. Design (*b*) is able to accommodate a volume of 251 cm^3. Design (*b*) is made in a minimalist and ventilated form. This is performed in order to the body has airflow so that the components in the body are not too fast to heat up. The same thing is conducted in design (*c*) which has dimensions of 164 x 115 x 30 mm. Design (*c*) is longer than the previous design. This is performed to provide a balance to the design (*c*) because it has a large angle between the two feet which reaches 65º. Designs (*a*) and (*b*) have angles at both feet of 60º and 40º. In addition, the dimensions of the design (*c*) are also formed to meet the needs of robot components, especially at the leg as the location of the servomotor. It has a longer arm than other types in its type. As a result, the design of the body must adjust to the need of the servo arm so that the servo can operate optimally. With dimensions of that size makes the body able to accommodate a volume of 260 cm^3 and has a total mass of 45 grams. Based on research objectives that require a minimalist and lightweight design, the design (*c*) meets these needs compared to designs (*a*) and (*b*).

Further, the body design used of this soft robot is based on analysis using the FEA where each body design is given a 400-gram load for each body (*a, b, c*). Based on the analysis of safety factors performed, the value of the safety factor of each body is strong enough to hold the load, especially for design (*a*) and (*c*). As for the inside of the body, there are four servomotors that should work in non-hot environmental conditions. Therefore, the design of the body (*c*) is chosen because the safety factor values are sufficient and there is an airflow to refrigerate the servomotors.

2.3. Electrical design

Some electrical components are selected according to the required specifications. For the actuator system motor-tendon drive, the DS215MG KST servo motor was chosen, and the Arduino Mega 2560 was used as the gait generation control computing center. For remote control, the robot uses two nRFL2401 media as a data transfer control medium for the transmitter and receiver. The most commonly used battery voltage is 3.7 volts (1 cell) and 7.4 volts (2 cells), so in this study, 500 mAH and 1000 mAH 2 cell batteries are used with an output of 7.4 V. The electric component used in the robot component is presented in Fig. 5.

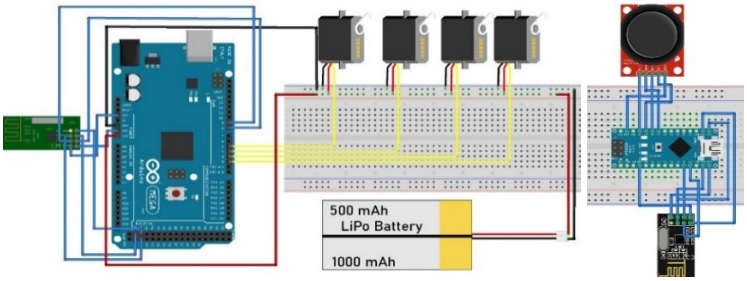

Fig. 5. Wiring for electrical components in the robot and remote control.

The utilized servo motor is the DS215MG KST micro servo type. Based on tests that have been carried out by giving a rotation angle command on the servo and measuring the resulted rotation angle of the output, the generated maximum error is $\pm 1^0$. The resulted errors from servo motor angle glitch and slip are not included in this study because the robot implements open-loop control based on the standard servo command (Pulse Width Modulation) to drive the servomotor that pulls the soft leg tendons to form a bending angle motion. The soft robot implements open-loop control by giving the signal input command in servomotor to bend and unbend the soft leg for terrestrial locomotion. The signal input commands of the proposed robot are generated using the Fourier series as a gait generation function. There is no sensor for position/orientation feedback control for the robot.

3. Gait Generation

In this study, the starfish movement patterns are studied based on the order of the foot movements. A previous study conducted by Trivedi et al. [3] showed that the pattern of starfish movements was with two legs walking and followed by three other legs, or vice versa. Then it is necessary to design movement patterns first and

develop a gait generation program that will be embedded as a robot motion controller in the microcontroller.

In the previous research, two types of gait strategy for the quadrupedal starfish soft robot prototype were undulating and ambulating. Undulating motion strategy is a strategy of robot motion by going forward using two rear actuators followed by two front actuators so that the resulting motion is similar to wave motion (undulate). While the ambulating motion strategy is a motion strategy where the robot moves with the opposite actuator (diagonal). The ambulating movement starts from the left rear actuator assisted by the right front actuator, then continues with the right rear actuator assisted by the front left actuator or starts from the opposite diagonal. But based on the results of the analysis obtained in terms of speed, undulating gait type is faster than ambulating type gait. Besides that, the servo also works lighter because in one cycle the gait type undulating servo moves only 1x gain, whereas for one cycle the gait type ambulating servo moves 1x gain plus 0.5x gain used. The gain itself is a large angle set for the movement of the servo motor in moving the soft leg of the robot.

In this study, the type of undulating gait is selected and implemented as the main-gait quadrupedal starfish soft robot in a driving movement to walk straight ahead. Then gait crawling was developed to adjust the quadrupedal starfish soft robot in adaptation to the environment to be able to pass an obstacle that prevents the movement of the robot. The undulating gait has a step like a bumpy motion. First, the four soft leg actuators move with 1x gain and then return to a stationary position with the body. This leads the servo re-calibrated to the zero-setting position (initial condition). The two soft leg rear actuators (right and left) move 1x gain causing contractions and body lift, then relax until the robot moves forward. The two soft leg front actuators (right and left) move 1x gain right after the two soft leg rear actuators relax, resulting in the contraction of the actuator. After that, the four actuators and body return to rest and are ready for the next cycle. As for the backward movement, then by changing the order from *a-b-c-d to a-c-b-d*. In the lateral movement to the right side, the two left-side actuators move first and followed by two right-side actuators. While for the movement to the left side, the two right-side actuators move first and are followed by two left-side actuators.

Gait crawling strategy has a step of walking in a standing condition. This motion strategy makes the robot can walk over the object underneath so that the robot does not need to change direction in moving forward. In the first step of gait crawling, the four actuators and the body are at rest, and then four actuators make 0.5x gain movements to make the robot stand up. The left rear actuator adds to its contraction so that it reaches 1x gain then while this actuator relaxes up to 0.5x gain, the right front actuator contracts to reach 1x gain and continues with relaxation up to 0.5x gain. In this condition, the robot is standing again, but the position of the two actuators is in front of the other two actuators. The right-rear actuator adds to its contraction so that it reaches 1x gain, while this actuator relaxes up to 0.5x gain. The front left actuator contracts to reach 1x gain and continues with relaxation up to 0.5x gain. This condition causes the robot to move forward perfectly while still standing. The four actuators are still in a 0.5-contraction state and are ready to perform sequences c and d to return to continuous movement. The undulating and crawling command signal can be seen in Fig. 6.

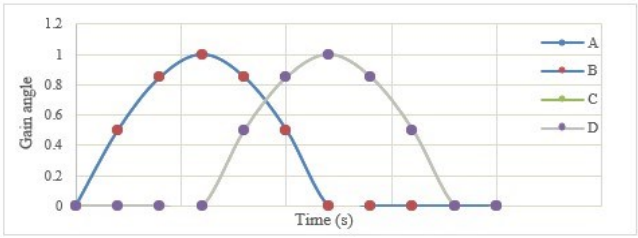

(a) Undulating.

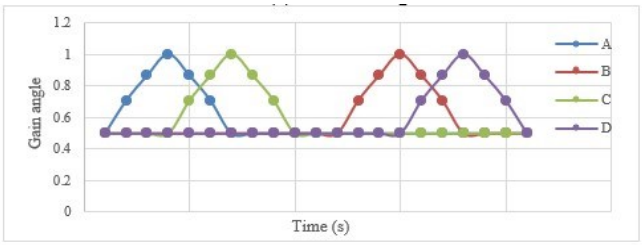

(b) Crawling.

Fig. 6. Two main gait patterns for one-step gait.

3.1. Gait pattern

A quadrupedal starfish soft robot certainly has a varied work environment, ranging from flat terrain with smooth surfaces, flat terrain with rough surfaces, terrain with small obstacles, and terrain with large obstacles that are difficult for the robot to pass. In order to the robot can past the various terrains, it is necessary to develop a gait motion strategy for the robot. The first step in developing a motion gait strategy is to generate multi-gait patterns, which contain the control of contraction and relaxation settings for each actuator on the soft robot. Contraction is a condition when the actuator moves, while relaxation is a condition where the actuator is stationary. The multi-gait pattern that will be applied to the robot in order to adapt to its environment is shown in Fig. 7.

Based on the multi-gait pattern in Fig. 7, it is known that the gait pattern of motion formed for terrains with smooth surfaces and rough surfaces is *dc-ba*, where the two rear actuators move together then followed by the two front actuators. For terrain with small obstacle, the pattern of motion that is formed is *a'b'c'd* '| *db* | *a'b'c'd'* | ca where the sign (') indicates the robot performs a contraction of 0.5x gain (maximum angle of servo) which is determined so that it stands up and can bypass small obstacles encountered. The second choice for this terrain is to implement the *dc-ba* | *cb-da* | *dc-ba* | *da-cb* | *dc-ba* gait movement pattern. The pattern enables the robot to move in a straightforward step - sliding left - straight forward - sliding right - straight forward, so that the obstacle can be passed by sliding the quadrupedal starfish soft robot to the side of the obstacle and then proceeding straight ahead to return to the forward movement. For terrain with an impassable obstacle, the proposed movement pattern is *da-cb* | *cb-da*, where the robot initially moves a right turn until its position is beside the 90º obstacle. The robot turns left of 90º so that the robot is in a position parallel to the obstacle and ready to move forward. Multi-gait strategies that are developed for various terrains are summarized in Table 2.

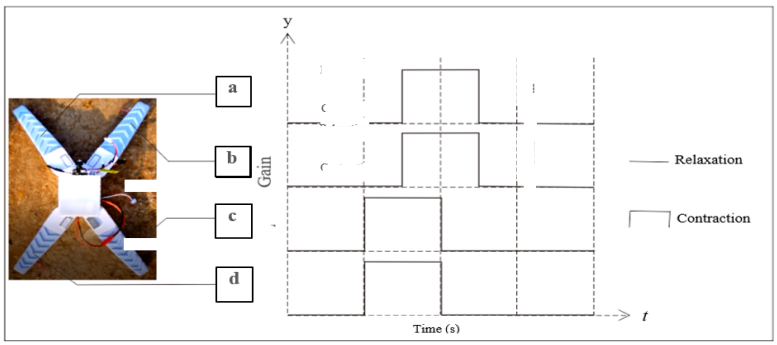

(a) Flat terrain.

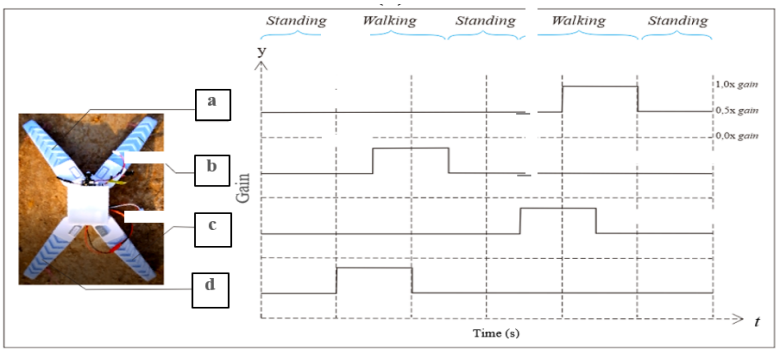

(b) First selected gait for small obstacle.

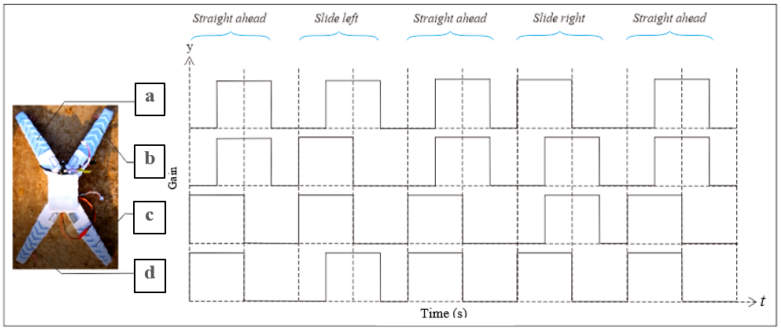

(c) Second selected gait for small obstacle.

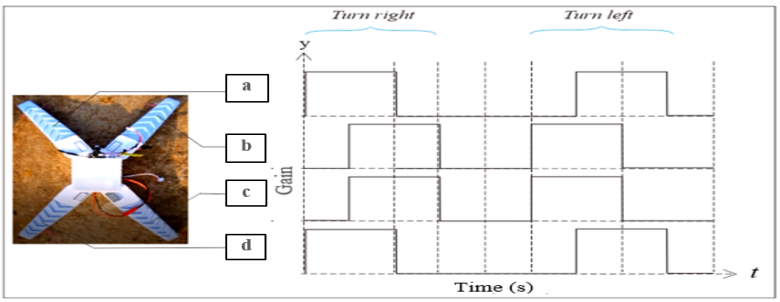

(d) impassable obstacle.

Fig. 7. Multi-gait pattern.

The complex undulating gait presented in Table 2 is a motion strategy that contains an undulating motion to move forward, undulating to shift to the left, and undulating to shift to the right. While the turning undulating strategy is a gait strategy where the robot makes a right turn so that it rotates 90º, then makes a left turn 90º with a sliding forward so that obstacles can be passed. Turning motion is almost the same as shifting but with a smaller angular value on one of the actuators.

Table 2. Gait strategy and soft leg sequence.

Environmental condition	Soft leg sequence	Gait strategy
Smooth terrain	*dc-ba*	Undulating
Rough terrain	*dc-ba*	Undulating
Small obstacle	*a'b'c'd'|d-b|a'b'c'd'|c-a or dc-ba|cb-da|dc-ba|da-cb|dc-ba*	Crawling or Complex undulating
Impassable obstacle	*da-cb|cb-da*	Turning undulating

3.2. Embedded gait pattern

The embedded gait pattern implemented in the proposed robot employs the equation from the Fourier series. Fourier series is selected because it is one of the periodic functions that can fit the gait motion for both undulating and crawling gait. In addition, by implementing this Fourier equation as the gait generation, the speed of robot motion will be more easily regulated by giving different values at the angular frequency (ω). Equation (1) shows the Fourier series equation of order 6 which is utilized to the gait generation of the robot's motion both on the undulating and crawling gaits. While the parameters used in the Fourier series can be summarized as in Table 3 that it can be obtained by using a curve fitting toolbox in MATLAB software. The sample points from undulating and crawling gaits as shown in Fig. 6 are exported in the curve fitting toolbox to obtain the parameters as summarized in Table 3 by using the Fourier series as curve fitting.

$$\begin{aligned} f(t) = \frac{a_0}{2} + a_1\cos(wt) + b_1\sin(wt) + a_2\cos(2wt) + b_2\sin(2wt) + \ldots \\ a_3\cos(3wt) + b_3\sin(3wt) + a_4\cos(4wt) + b_4\sin(4wt) + \ldots \\ a_5\cos(5wt) + b_5\sin(5wt) + a_6\cos(6wt) + b_6\sin(6wt) \end{aligned} \quad (1)$$

The right and left turn of the quadrupedal starfish soft robot has the same Fourier equation except for different phases. The two movements of the gait generations use the sixth-order Fourier series. The difference between these two movements lies in the curve fitting graph and the Fourier coefficients of the generated gait. The Fourier coefficient value on the right soft legs (*b, c*) for the turn right movement has the same value as the front actuator coefficient for the forward movement. In the right turn, the Fourier coefficient which has the same value is the right front (*b*) and the right rear (*c*).

The coefficient value of the right foot on the right turn motion can be implemented to the left actuator on the left-turn movement. Similar to the right Fourier coefficient, the left Fourier coefficient has the same value as the forward movement. The value of the left Fourier coefficient for the right turn motion has the same as the value of the actuator coefficient behind the forward movement. The value of the left Fourier coefficient can also be implemented to the right actuator

for left-turn movements. The implemented gait sequence of the gain angle for each servomotor on longitudinal, lateral and turning left/right are summarized in Table 4. Parameters in Table 4 are obtained experimentally for the optimum gait to walk in the longitudinal, lateral and turning way.

Table 3. Fourier coefficient of undulating gait for forward/backward walk with $\omega = 3.11$ rad/s.

Fourier Coefficient	Forward walk				Backward walk			
	Leg a	Leg b	Leg c	Leg d	Leg a	Leg b	Leg c	Leg d
a_0	0.3661	0.3661	0.3664	0.3664	0.3661	0.3661	0.3664	0.3664
a_1	-0.0004	-0.0004	4.08×10^5	4.08×10^5	-0.0004	-0.0004	$4.08\text{x}10^5$	$4.08\text{x}10^5$
b_1	6.13×10^5	6.13×10^5	-4.4×10^5	-4.4×10^5	6.13×10^5	6.13×10^5	$-4.3\text{x}10^5$	$-4.3\text{x}10^5$
a_2	-0.2258	-0.2258	0.3769	0.3769	-0.2258	-0.2258	0.3769	0.3769
b_2	0.4625	0.4625	-0.3501	-0.3501	0.4625	0.4625	-0.3501	-0.3501
a_3	-0.0003	-0.0003	-8.5×10^6	-8.5×10^6	-0.0003	-0.0003	$-8.5\text{x}10^6$	$-8.5\text{x}10^6$
b_3	0.0002	0.0002	-0.0001	-0.0001	0.0002	0.0002	-0.0001	-0.0001
a_4	-0.0788	-0.0788	0.0097	0.0097	-0.0780	-0.0780	0.0097	0.0097
b_4	-0.0994	-0.0994	0.1264	0.1264	-0.0994	-0.0994	0.1264	0.1264
a_5	-0.0002	-0.0002	-9.4×10^5	-9.4×10^5	-0.0002	-0.0002	$-9.4\text{x}10^5$	$-9.4\text{x}10^5$
b_5	0.0003	0.0003	-0.0001	-0.0001	0.0003	0.0003	-0.0001	-0.0001
a_6	-0.0441	-0.0441	-0.0277	-0.0277	-0.0440	-0.0440	-0.0277	-0.0277
b_6	0.0103	0.0103	0.0353	0.0353	0.0103	0.0103	0.0353	0.0353

Table 4. The implemented sequence of gain angle of each servomotor angle command in each soft leg.

Servomotor angle in soft leg	Longitudinal walk (deg)		Lateral walk (deg)		Turning (deg)	
	Forward	Backward	Right	Left	Right	Left
a	110 (1st)	120 (3rd)	130 (2nd)	130 (1st)	130 (2nd)	130 (1st)
b	130 (2nd)	120 (4th)	130 (4th)	130 (3rd)	130 (4th)	130 (3rd)
c	120 (3rd)	115 (1st)	130 (1st)	130 (2nd)	90 (1st)	90 (2nd)
d	120 (4th)	130 (2nd)	130 (3rd)	130 (4th)	130 (3rd)	130 (4th)

After developing the multi-gait strategy for the proposed soft robot, the gait pattern as presented in Fig. 6 is modelled mathematically using the Fourier series equation as expressed in the Eq. (1). The gait pattern is developed under MATLAB/Simulink environment. The developed model of the gait generation block diagram in Simulink environment is presented in Fig. 8. The block also contains the embedded program of wireless communication between the soft robot and the joystick command/host computer.

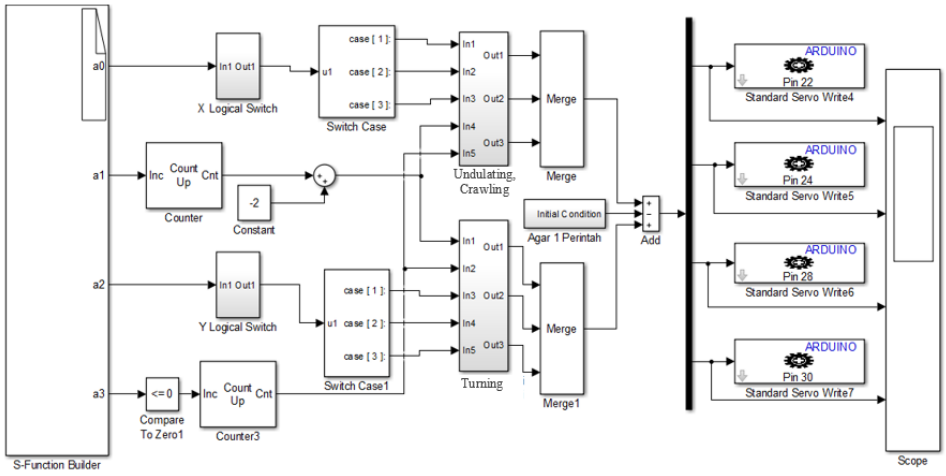

Fig. 8. Main level system of embedded multi-gait generation of the proposed soft robot in Arduino microcontroller.

4. Results and Discussion

A proposed quadrupedal starfish soft robot with a minimalist and lightweight design, as well as the addition of a camera to assist a pilot know the real-time conditions around the robot. The quadrupedal starfish soft robot was successfully designed in the form of an X configuration with the dimensions of 350×230×52 mm. Figure 9 shows the results of a developed quadrupedal starfish soft robot.

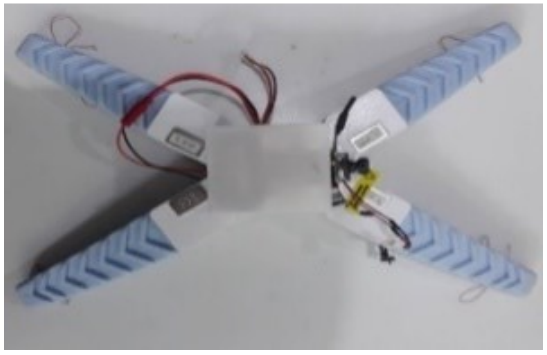

Fig. 9. Quadrupedal starfish soft robot prototype.

4.1. Experimental test in various terrains

To find out the effectiveness of the proposed gait generation strategy applied to the quadrupedal starfish soft robot, an experimental test was carried out. This test is carried out on predetermined fields, namely flat terrain with both smooth and rough surfaces, fields with a small obstacle, and field with impassable obstacles.

4.1.1. Smooth terrain

In this test, the robot is tested to walk using the undulating gait strategy on two flat surfaces. Based on the test results, it can be seen that the undulating strategy applied

to the two flat terrains on smooth and rough surfaces has been successfully carried out and the robot can walk on the surface of the carpet and paving block. However, there is a difference in the time required to do one-step of walking, where on the terrain with a smooth surface takes 2.17 seconds, while on a rough surface is 2.14 seconds. Figure 10 shows the results of experimental testing on smooth and rough flat fields.

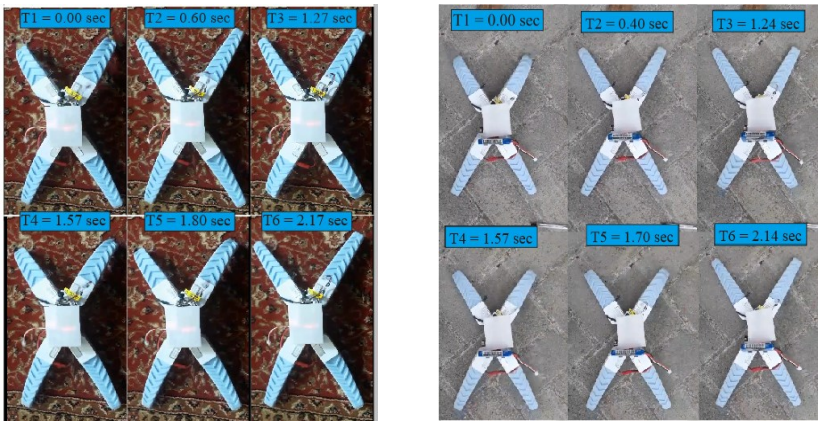

(a) Smooth surface. **(b) Rough surface.**

Fig. 10. Experimental testing on flat terrain.

4.1.2. Terrain with small obstacle

In this test, the robot is tested to be able to walk through a small obstacle. The obstacle in this test is a bottled water. The gait strategies applied in this research are complex undulating and crawling gait. Based on the results, the successful gait strategy is a complex undulating gait. The crawling gait strategy failed to be implemented because of the mass and dimensions of the robot is large, so that the movement of the robot in stepping over obstacles experienced interference. Figure 11 shows the results of experimental tests on the terrain with a small obstacle.

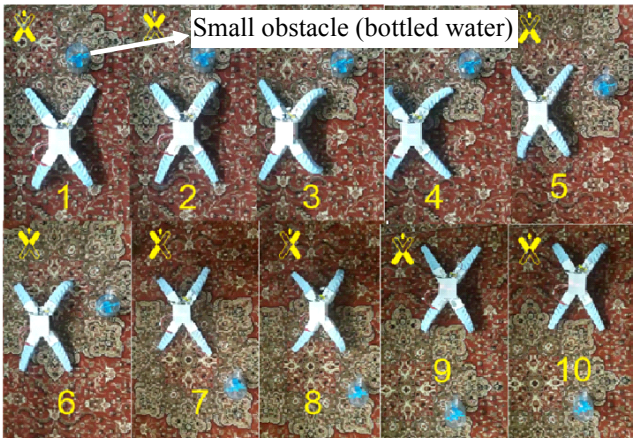

Fig. 11. The experimental test on flat terrain with a small obstacle.

4.1.3. Terrain with impassable obstacle

In this test, the robot is tested to walk on a field with large obstacles that are difficult to pass by a robot (impassable obstacle). The turning undulating gait is selected in this test. Based on the test results, the turning undulating strategy was successfully applied to the robot to pass an impassable object in the form of a 7 cm high stack of paper. The robot can pass the obstacle by turning right and then turning left so that the robot's position is next to the obstacle as shown in Fig. 12.

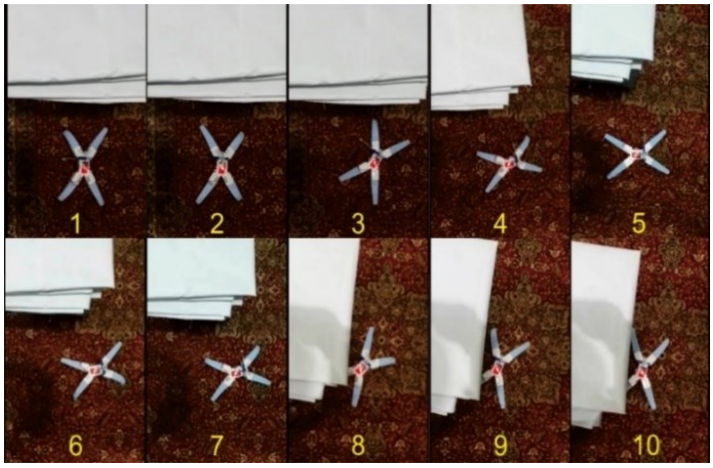

Fig. 12. The experimental test on flat terrain with an impassable obstacle.

4.2. Trajectory, displacement and speed

4.2.1. Walking trajectory

In this test, the walking trajectory test is performed to the robot for walking both forward and backward. This test is conducted to find out how far the quadrupedal starfish soft robot deviates from the straight line of the track. The test was carried out on three different trajectories namely carpet trajectory, asphalt trajectory, and paving block trajectory. Walking trajectory testing is carried out on a 500 mm long track for forward and backward walking movements. Figure 13 shows the results of the walking trajectory of the robot test when given by angular frequency inputs of 2.1 rad/s, 3.1 rad/s, 4.1 rad/s, 5.1 rad/s, and 6.1 rad/s to the Fourier series as expressed in the Eq. (1).

Based on Fig. 13, it can be concluded that the greater the angular frequency input, the greater the error in the straight-line track that occurs in the quadrupedal starfish soft robot. It is also known from the result that the movements that produce relatively small trajectory deviations occur at angular frequencies between 2 rad/s to 4 rad/s. In addition, the most ideal movement occurs in the smooth trajectory on the carpet. While the results of trajectory tests on backward movement tend to have varied error values between right and left. The path errors that arise in walking trajectory from the soft robot walking occur because of the imperfect manufacturing process of the soft leg.

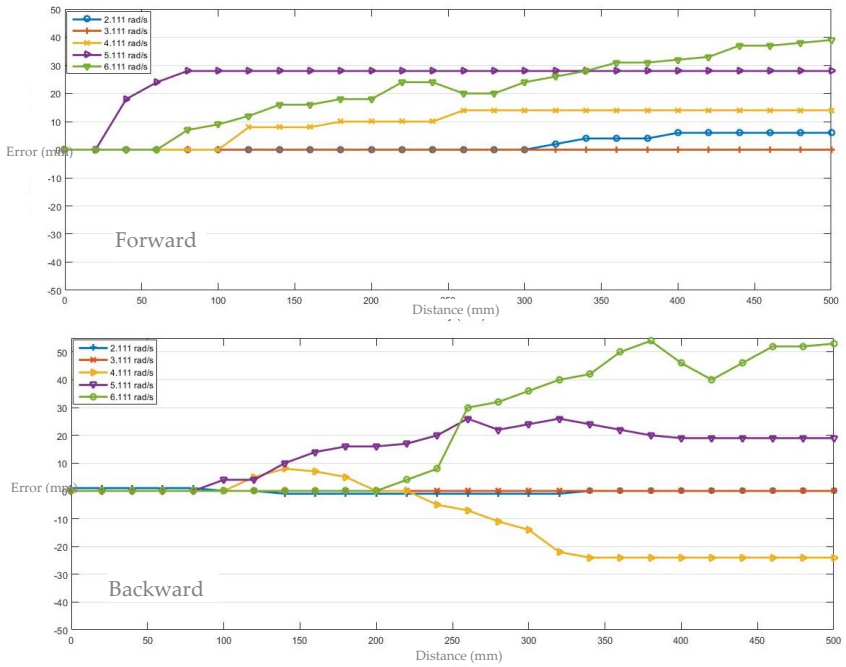

(a) Variation of trajectory test on carpet.

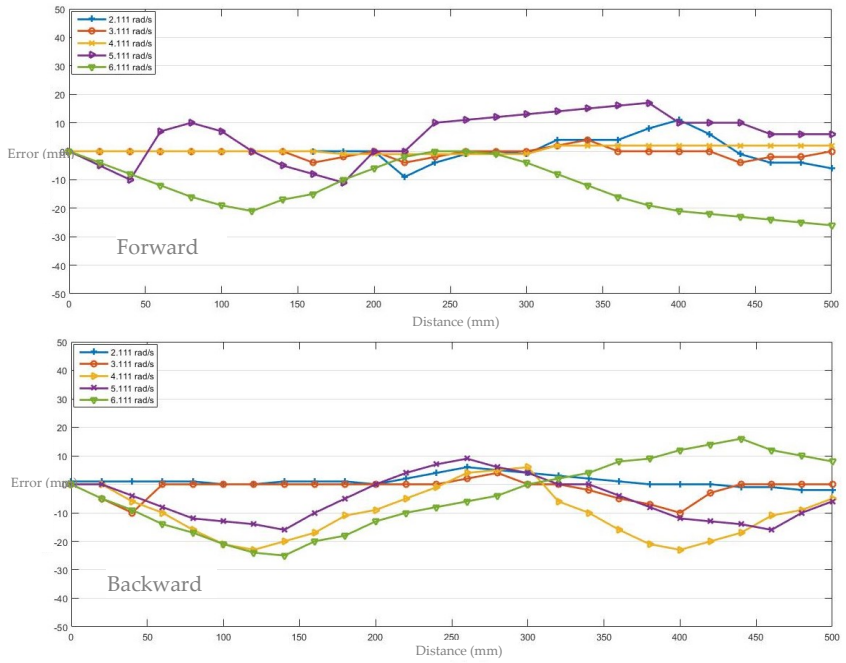

(b) Variation of trajectory test on asphalt.

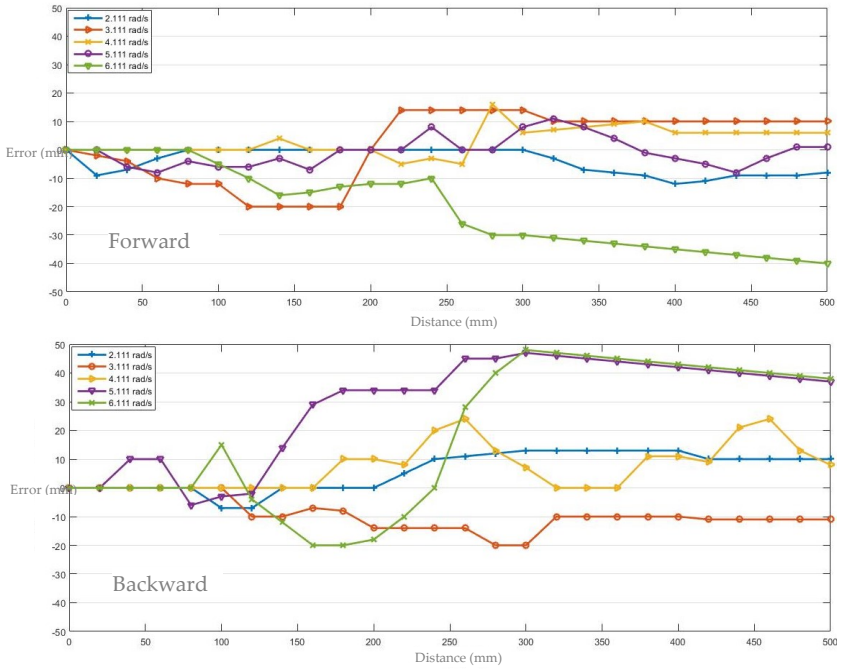

(c) Variation of trajectory test on paving block.

Fig. 13. Trajectory test.

Based on test result, the resulted deviation from the straight-line trajectory depends on (i) terrain type (soft or rough surface), (ii) angular frequency of the given Fourier series, (iii) the uneven bending angle resulting from each soft tendon leg caused by the uneven characteristics of the soft leg material during the manufacturing process. Because the distance is plotted from 0 mm to 500 mm, the deviation looks like constant deviation in certain increments. However, when the robot walks more than 500 mm, the resulted deviation is no longer constant but there is a change in the deviation even though the value is quite small. The robot is tested to walk on carpet, asphalt, and paving block without any external disturbances such as gust, and noisy environment. The gait of the robot implements the same gait of the Fourier equation with the same coefficients and angular frequency, but it uses different phase angles for forward and backward walk.

4.2.2. Displacement and velocity

In flat environmental conditions of terrain with smooth surfaces and rough surfaces, the gait strategy used in this test is undulating gait with a dc-ba gait pattern. By moving the robot straight forward to walk as far as 500 mm, data collection can be done to find out how many the speed ratio of the quadrupedal starfish soft robot is for both fields and how many the number of steps taken and the travel time to reach that distance. In this test the robot's mileage, and the time taken by the robot after a distance of 500 mm, and the number of steps of the robot during walking as far as 500 mm are measured and recorded for the study of the displacement and linear velocity of the robot. The surfaces tested in this study were carpet, paving block, tile floor, and asphalt.

Based on the test results, the displacement of the robot on the tile floor is very small because, at an angular velocity of 5.1 rad / s and 6.1rad / s, a slip occurs which causes the robot to move very small in each step. The displacement value that occurs in robots in fields with smooth surfaces and rough surfaces has a significant difference. On fields with smooth surfaces, the displacement value is small, whereas on fields with rough surfaces the value is higher. On terrain with rough surfaces, the surface conditions are uneven, so the displacement value of the robot is fluctuating. The displacement test results are presented in Fig. 14.

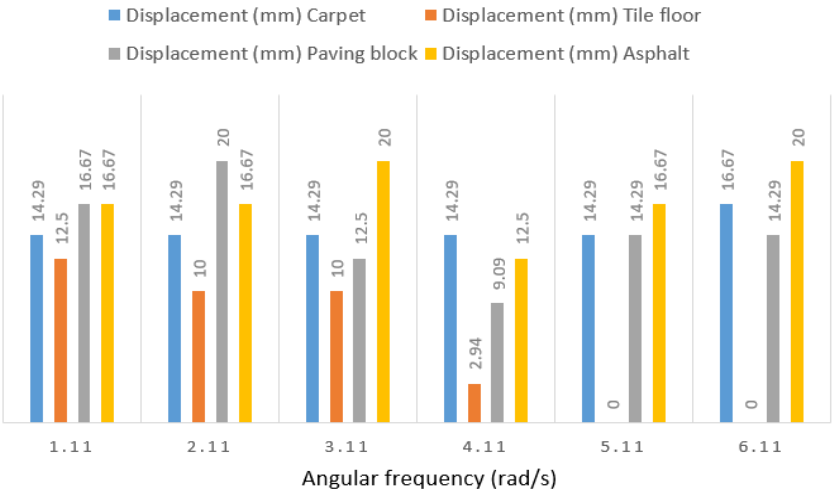

Fig. 14. Body displacement for each step on several surfaces.

From all the measurement results obtained, the linear velocity value of the quadrupedal starfish soft robot can be calculated in each field. The velocity values on terrain with rough surfaces are greater than those on the terrain with smooth surfaces, with a value of 17.36 mm/s for asphalt and 14.29 mm/s for paving blocks. While the velocity value on the smooth surface flat surface (carpet) is smaller, only reaching 14.18 mm/s. This is because there is a slip that occurs on a flat surface smooth surface. Figure 15 shows a comparison graph of the velocity values in each field for an angular frequency of 2.11 rad/s and 3.11 rad/s.

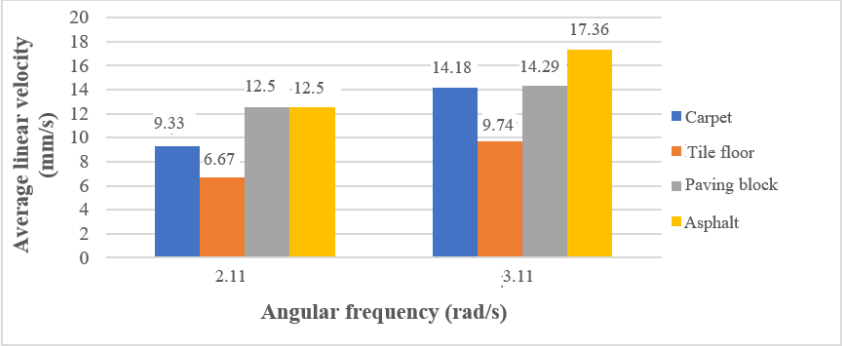

Fig. 15. Comparison of the average body linear velocity for each terrain.

4.3. Loading test

A loading test is performed to determine the maximum weight that can be lifted by the robot when it walks. This test is conducted by giving a load in stages starting from the weight of 51 grams to the weight of the load where the robot is not able to stand carrying the load. The result of this test is that the robot can only carry a maximum load of 400 grams. Figure 16 shows the visualization of loading test on the quadrupedal starfish soft robot. Test images show that the robot cannot carry a payload that weighs more than 400 grams.

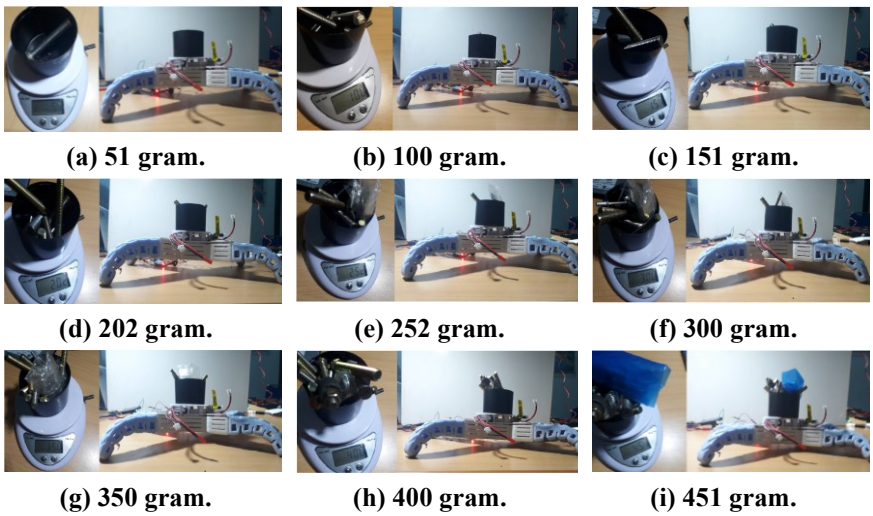

(a) 51 gram. **(b) 100 gram.** **(c) 151 gram.**

(d) 202 gram. **(e) 252 gram.** **(f) 300 gram.**

(g) 350 gram. **(h) 400 gram.** **(i) 451 gram.**

Fig. 16. Visualization of loading test on quadrupedal starfish soft robot against loads.

4.4. Wireless communication range test

One of the tests that need to be executed is the wireless communication range used on the quadrupedal starfish soft robot. This test is performed with the condition of the battery fully charged and partially used to find out how far the maximum range if the condition of the battery is full and the changes that occur if the capacity/ voltage of the battery decreases. Figure 17 shows the test scheme and the effect of battery capacity conditions on the range of wireless communication.

(a) Testing scheme. **(b) Effect of battery capacity against distance.**

Fig.17. Test range of wireless communication.

From the results of this test, it was found that the maximum distance for wireless communication on the condition of a 100 % battery capacity is 46 m. The maximum distance of wireless communication that can be achieved is 25 m on 50 % battery capacity. Whereas in wireless communication for video, the maximum range that can be achieved from the video transmitter and video receiver in displaying real-time video is 60 m.

5. Conclusions

In this study, a prototype of a quadrupedal starfish soft robot has been successfully developed using motor-tendon type actuator. Gait generation strategy is generated by implementing Fourier series. By using the Fourier series as a gait generation on the robot, the walking speed of the soft robot can be regulated easily. The quadrupedal like-starfish soft robot has an X configuration with dimensions of 350 x 230 x 52 mm and a total robot weight of 545 grams. The undulating gait motion strategy was successfully applied to the robot to walk on flat terrain with both smooth and rough surfaces. The robot can walk using complex undulating gait to pass through a field with small obstacles and turning undulating on a field with impassable obstacles. Based on the results of the trajectory tests that have been carried out, it can be concluded that the higher the speed of the robot, the higher the deviation value to the straight line. A small error is generated when the angular frequency in the Fourier series is 2.11 rad/s to 4.11 rad/s. On terrain with smooth surfaces, the robot moves slower than walking on the terrain with rough surfaces. This is can be influenced by slippage on terrain with a smooth surface and has a relatively smaller displacement value. The robot can run with a load of 400 grams, and the range of wireless control communication can be reached as far as 46 m.

Acknowledgement

The authors wish to thank Diponegoro University for the international scientific publication grand received (No. 474-98/UN7.P4.3/PP/2019) for supporting the funding of this research.

Nomenclature

$a_{0,1,2....}$	Fourier coefficient
$b_{0,1,2....}$	Fourier coefficient
f(t)	Fourier series regression approximation function
t	Time, s

Greek Symbols

ω	Angular frequency, rad/s

Abbreviations

CoG	Centre of Gravity
RTV	Room-Temperature-Vulcanizing

References

1. Shepeherd, R.F.; Ilievski, F.; Choi, W.; Morin, S.A.; Stokes, A.A.; Mazzeo, A.D.; Chen, X.; Wang, M.; and Whitesides, G.M. (2011). Multi-gait soft robot. *Proceedings of the National Academy of Sciences.* United States, 108(51), 20400-20403.
2. Trimmer, B.A.; Lin, H.; Baryshyan, A.; Leisk, G.G.; and Kaplan, D.L. (2012). Towards a biomorphic soft robot: Design constraints and solutions. *Proceedings of the Fourth IEEE RAS/EMBS International Conference on Biomedical Robotics and Biomechatronics (BioRob)*. Rome, Italy, 599-605.
3. Trivedi, D.; Rahn, C.D.; Kier, W.M.; and Walker, I.D. (2008). Soft robotics: Biological inspiration, state of the art, and future research. *Bionics and Biomechanics*, 5(3), 99-117.
4. Wang, T.; Ge, L.; and Gu, G. (2018). Programmable design of soft pneu-net actuators with oblique chambers can generate coupled bending and twisting motions. *Sensors and Actuators A: Physical,* 271, 131-138.
5. Mosadegh, B.; Polygerinos, P.; Keplinger, C.; Wennstedt, S.; Shepherd, R.F.; Gupta, U.; Shim, J.; Bertoldi, K.; Walsh, C.J.; and Whitesides, G.M. (2014). Pneumatic networks for soft robotics that actuate rapidly. *Advance Function Material*, 24, 2163-2170.
6. Tolley, M.T.; Shepherd, R.F.; Mosadegh, B.; Galloway, K.C.; Wehner, M.; Karpelson, M.; Wood, R.J.; and Whitesides, G.M. (2014). A resilient, untethered soft robot. *Soft Robotics*, 1(3), 213-223.
7. Stokes, A.A.; Shepherd, R.F.; Morin, S.A.; Ilievski, F.; and Whitesides, G.M. (2014). A hybrid combining hard and soft robots. *Soft Robotics*, 1(1), 70-74.
8. Mao, S.; Dong, E.; Jin, H.; Xu, M.; Zhang, S.; Yang, J.; and Low, K.H. (2014). Gait study and pattern generation of a starfish-like soft robot with flexible rays actuated by SMAs. *Journal of Bionic Engineering*, 11, 400-411.
9. Akbari, S.; Sakhaei, A.H.; Panjwani, S.; Kowsari, K.; Serjourei, A.; and Ge, Q. (2019). Multimaterial 3D printed soft actuators powered by shape memory alloy wires. *Sensors and Actuators A: Physical,* 290, 177-189.
10. Jin, H.; Dong, E.; Alici, G.; Mao, S.; Min, X.; Liu, C.; Low, K.H.; and Yang, J. (2016). A starfish robot based on soft and smart modular structure (SMS) actuated by SMA wires. *Bioinspiration & Biomimetics*, 11(5), 056012.
11. Mao, S.; Dong, E.; Zhang, S.; Xu, M.; and Yang, J. (2013). A new soft bionic starfish robot with multi-gaits. *Proceedings of the 2013 IEEE/ASME International Conference on Advanced Intelligent Mechatronics*. Wollongong, Australia, 1312-1317.
12. Liu, C.; Dong, E.; Xu, M.; Alici, G.; and Yang, J. (2018). Locomotion analysis and optimization of actinomorphic robots with soft arms actuated by shape memory alloy wires. *International Journal of Advanced Robotic Systems*, 15(4), 1-14.
13. Mao, S.; Dong, E.; Jin, H.; Xu, M.; and Low, K.H. (2016). Locomotion and gait analysis of multi-limb soft robots driven by smart actuators. *Proceedings of the 2016 IEEE/RSJ International Conference on Intelligent Robots and Systems (IROS)*. Daejeon, South Korea, 2438-2443.

14. Tang, X.; Li, K.; Liu, Y.; Zhou, D.; and Zhao, J. (2019). A soft crawling robot driven by single twisted and coiled actuator. *Sensors and Actuators A: Physical,* 291, 80-86.
15. Vikas, V.; Cohen, E.; Grassi, R; Sozer, C.; and Trimmer, B. (2016). Design and locomotion control of a soft robot using friction manipulation and motor-tendon actuation. *IEEE Transactions on Robotics,* 32(4), 949 - 959.
16. Umedachi, T.; Vikas, V.; and Trimmer, B.A. (2016). Softworms: the design and control of non-pneumatic, 3D-printed, deformable robots. *Bioinspiration & biomimetics*, 11(2), 1-16.
17. Manwell, T.; Guo, B.; Back, J.; and Liu, H. (2018). Bioinspired setae for soft worm robot locomotion. *Proceedings of the 2018 IEEE International Conference on Soft Robotics (RoboSoft)*. Livorno, Italy, 54-59.
18. Vikas, V.; Cohen, E.; Grassi, R.; Sozer, C.; and Trimmer, B. (2016). Design and locomotion control of a soft robot using friction manipulation and motor-tendon actuation. *IEEE Transactions on Robotics,* 32(4), 949-959.
19. Donatelli, C.M.; Serlin, Z.T.; Echols-Jones, P.; Scibelli, A.E.; Cohen, A.; Musca, J.M.; Rozen-Levy, S.; Buckingham, D.; White, R.; and Trimmer, B.A. (2017). Soft foam robot with caterpillar-inspired gait regimes for terrestrial locomotion. *Proceedings of the 2017 IEEE/RSJ International Conference on Intelligent Robots and Systems (IROS)*. Vancouver, Canada, 476-481.
20. Kastor, N.; Mukherjee, R.; Cohen, E.; Vikas, V.; Trimmer, B. A.; and White, R.D. (2020). Design and manufacturing of tendon-driven soft foam robots. *Robotica*, 38(1), 88-105.
21. Liu, J.; Hong, W.; and Xie, L. (2017). Design of a soft crawling robot with turning function. *Proceedings of the 2017 IEEE International Conference on Real-time Computing and Robotics (RCAR)*. Okinawa, Japan, 1-4.
22. Lee, C.; Kim, M.; Kim, Y. J.; Hong, N.; Ryu, S.; Kim, H.J.; and Kim, S. (2017). Soft robot review. *International Journal of Control, Automation and Systems*, 15(1), 3-15.
23. Loepfe, M.; Schumacher, C. M.; Lustenberger, U.B.; and Stark, W.J. (2015). An Untethered, Jumping Roly-Poly Soft Robot Driven by Combustion. *Soft Robotics,* 2(1), 33 - 41.
24. Munadi, M.; Ariyanto, M.; Setiawan, J.D.; Purwanto, E.; Akbar, M.A.; Fauzi, A.H.; and Setiawan, M.N. (2018). Design and manufacturing of motor-tendon actuator for a soft starfish-like robot. *Proceedings of the 2018 3rd International Seminar on Sensors, Instrumentation, Measurement and Metrology (ISSIMM)*. Jakarta, Indonesia, 15-20.